Trapping Single Polar Molecules in SiC Nanomesh *via* Out-of-Plane Dipoles

Han Huang,[†,‡,*] Swee Liang Wong,[†,§] Jiatao Sun,[⊥] Wei Chen,[†,‡,§,⊥] and Andrew Thye Shen Wee[†,‡,§,*]

[†]Department of Physics, and [‡]Graphene Research Centre, National University of Singapore, 2 Science Drive 3, 117542, Singapore, [§]NUS Graduate School for Integrative Sciences and Engineering, National University of Singapore, 28 Medical Drive, 117456, Singapore, and [⊥]Department of Chemistry, National University of Singapore, 3 Science Drive 3, 117543, Singapore

ABSTRACT

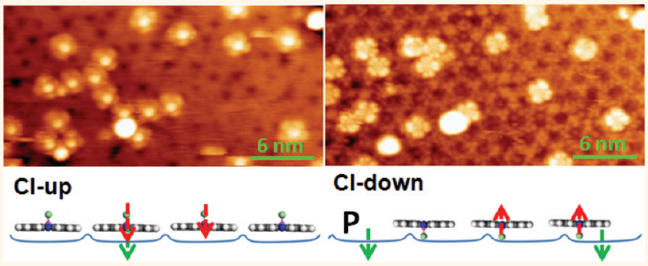

The self-assembly of nonplanar chloroaluminum phthalocyanine (ClAlPc) molecules as well-ordered single-molecule dipole arrays on the silicon carbide (SiC) nanomesh substrate was investigated using low temperature scanning tunneling microscopy. ClAlPc exclusively adsorbs in the center of the SiC nanomesh holes with its inherent dipole (from Cl to Al) pointing toward the substrate. The dipole can be inverted by a positively biased tip with a threshold tip voltage of 3.3 V. We deduce that the interaction between the intrinsic dipole of ClAlPc and the periodic out-of-plane component of the surface dipole on the SiC nanomesh plays a significant role in the dipole array formation.

KEYWORDS: scanning tunneling microscopy · chloroaluminum phthalocyanine · SiC nanomesh · surface dipole · epitaxial graphene

Molecular electronics[1] is a promising alternative paradigm to conventional electronics to meet the demand for device miniaturization. To fabricate single molecule devices, a first step is to understand and control the formation of large scale well-ordered single-molecule arrays with desired functionality. To retain the pristine functions of molecules, it is necessary to assemble molecules on surfaces without forming strong covalent bonds, such as on two-dimensional (2D) supramolecular porous networks,[2−4] on dislocation networks,[5] or on electronically self-patterned single-crystalline Al_2O_3 thin film on NiAl(100).[6,7] Inert 2D atomically thin films such as the hexagonal boron nitride (*h*-BN) on transition metal surfaces[8,9] have been shown to be promising templates for single-molecular arrays, for example, naphthalocyanine[8] and copper phthalocyanine (CuPc).[9] Whereas naphthalocyanine molecule attaches at the center of the *h*-BN nanomesh hole,[8] CuPc molecule is randomly shifted off the center of the corresponding host hole.[9] This has been attributed to in-plane components of surface dipole rings of the *h*-BN nanomesh.

The $(6\sqrt{3} \times 6\sqrt{3})R30°$ reconstructed SiC (0001) surface,[10] also known as SiC nanomesh[11] (hereafter, SiC nanomesh), resembles a quasi-honeycomb structure with an average side length close to 1.85 nm, as shown in the filled state STM image and the corresponding fast Fourier transform (FFT) pattern in Figure 1a. It comprises a single graphene-like carbon layer which is partially covalently bonded to a truncated SiC(0001) surface,[12−16] as shown in the models in Figure 4d and Supporting Information, Figure S1. It can be electronically decoupled to be quasi-free-standing epitaxial graphene (EG).[17−22] The corrugation of the carbon layer is calculated to be close to 0.12 nm,[15] in good agreement with our previous STM measurements.[11] The boundaries of the nanomesh correspond to regions where C atoms are not commensurate with SiC and hence are suspended on top of it without any covalent bond formation; while the holes correspond to regions where the C-honeycomb is covalently bonded to the underlying SiC *via* Si−C σ-bonds.[14] Such covalent bonding breaks the hexagonal network of π-orbitals but preserves the σ-bonds of sp^2 hybridization,[13] making the SiC nanomesh semiconducting. The resulting charge transfer from SiC to the corrugated graphene-like carbon layer is uneven and is localized in the hole regions close to the interface,[13,14] which results in a perpendicular dipole in each hole (see Supporting Information (SI)). Our previous study has demonstrated that SiC nanomesh is a good template for CuPc self-assembled arrays,

* Address correspondence to phyhh@nus.edu.sg, phyweets@nus.edu.sg.

Received for review January 17, 2012 and accepted February 23, 2012.

Published online February 28, 2012
10.1021/nn300258b

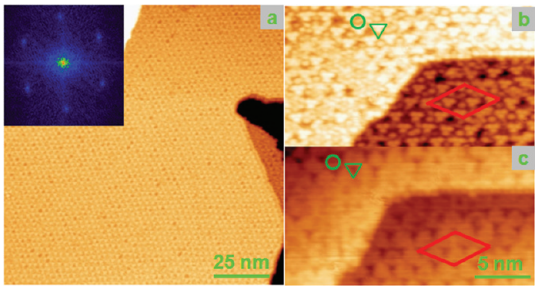

Figure 1. (a) Typical large scale STM image (V_T = 1.5 V) and the corresponding FFT pattern (inserted) showing the SiC nanomesh in quasi-hexagonal symmetry with a periodicity of ~1.85 nm. High resolution STM images, (b) (+) and (c) (−), from the same area but at opposite tip bias polarities showing the characterization of SiC nanomesh. The dark triangles in panel b correspond to the down-pointing trimers in panel c (labeled by green triangles), indicating that the holes of nanomesh (labeled by green circles) are featureless at negative tip bias. The unit cell of $(6\sqrt{3} \times 6\sqrt{3})R30°$ superstructure is marked by a red diamond.

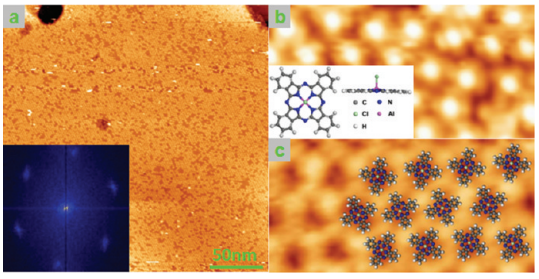

Figure 2. (a) Large scale STM image (V_T = −2.60 V) of ~0.85 ML ClAlPc on SiC nanomesh and corresponding FFT pattern (inserted) showing a long-range ordered single ClAlPc molecular array with quasi-hexagonal symmetry in a periodicity of ~1.85 nm. (b) Enlarged STM image (V_T = −2.83 V) showing all the ClAlPc in Cl-up configuration. Top view and side view of the molecular structure of ClAlPc are inserted. (c) Proposed model for ClAlPc molecules on SiC nanomesh.

but not for pentacene.[23] Here, we use a dipole molecule to elucidate the template self-assembly mechanism.

In this contribution, we use low temperature scanning tunneling microscopy (LT-STM) to investigate the formation of well-ordered single-molecular arrays of chloroaluminum phthalocyanine (ClAlPc) on a SiC nanomesh template, as well as demonstrate positively biased-STM-tip-induced molecular dipole orientation inversion. ClAlPc has an electric dipole moment pointing from a Cl atom to Al atom, perpendicular to the phthalocyanine plane (*cf*. structure in Figure 2b inset).[24] As deposited, ClAlPc molecules exclusively adsorb in the hole center of the SiC nanomesh template with their Cl-atoms pointing toward the vacuum. After several scans at tip biases around 3.3 V, the molecules in the scanned area were inverted with their Cl atoms now pointing to the substrate and shifted off-center and closer to the nanomesh boundaries. The out-of-plane components of the surface dipoles of the SiC nanomesh are believed to play a key role in the accommodation

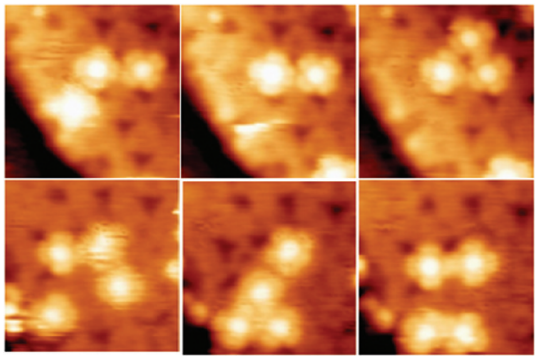

Figure 3. Series of molecularly resolved STM images (7.5 × 7.5 nm^2, V_T = −2.76 V) of 0.1 ML ClAlPc on the SiC nanomesh from the same area showing the hopping of the ClAlPc molecules between the holes of the SiC nanomesh.

of single ClAlPc molecules and the formation of such dipole arrays.

RESULTS AND DISCUSSION

Figure 1panels b and c show high resolution STM images of the SiC nanomesh at opposite tip bias polarities (b, 1.5 V; c, −1.5 V). There are two types of structural units dominating the surface in Figure 1b. One is the down-pointing trimer (highlighted by a green triangle), and the other is a single or double protrusion between the trimers (highlighted by a green circle). In Figure 1c, both structural units are observed to be significantly different. The former appears as dark triangles and the latter as irregular shaped units with a weak corrugation in a hexagonal geometry. In addition to the two above-mentioned features, there are several other types of structural units on SiC nanomesh reported in refs 12 and 25. The two types shown here correspond to Types C and E in ref 12, respectively. Type C is at the corner of a nanomesh and Type E is in the hole center of a nanomesh. A unit cell of $(6\sqrt{3} \times 6\sqrt{3})R30°$ reconstruction is marked on both panels, respectively, with a red diamond.

Upon depositing ~0.85 monolayer of (ML, where 1 ML refers to the coverage of one ClAlPc molecule per nanomesh hole) ClAlPc, a well-ordered single molecular array was observed on the SiC nanomesh, as shown in Figure 2a. The corresponding FFT pattern inserted at the lower left corner of Figure 2a shows a hexagonal symmetry with an averaged periodicity of ~1.85 nm, the same as that of the SiC nanomesh. The intermolecular distance is much larger than that close-packed ClAlPc on HOPG of 1.51 nm,[26] suggesting negligible interaction between neighboring ClAlPc molecules. The ClAlPc image resembles a protrusion with four equivalent lobes in the close-up STM images as shown in Figures 2b, 3, and 4b, which indicates that the phthalocyanine plane of ClAlPc lies flat on SiC nanomesh with its Cl-atom pointing to vacuum (hereafter, Cl-up configuration). Such growth behavior is

significantly different from that on HOPG,[24,26] where ClAlPc grows in a bilayer mode. The difference is discussed in detail later.

Figure 3 shows a series of molecularly resolved empty state STM images of 0.1 ML ClAlPc on the SiC nanomesh from the same area. The images evidence molecular hopping between specific sites on the SiC nanomesh, which is induced by either thermal activation or repulsive tip−molecule interaction at negative tip bias. Close inspection reveals that all the ClAlPc molecules are surrounded by three Type C structural units; that is, they are adsorbed on top of the Type E structural units. This indicates that the center of the molecule exactly locates at the center of a host nanomesh hole. A proposed model of ClAlPc on SiC nanomesh is shown in Figure 2c.

Simultaneous images of filled states with ClAlPc in Cl-up configuration and mesh-like structure of SiC nanomesh were not obtained. We attribute this to the strong attractive interaction between a positively biased tip and Cl-up ClAlPc, which perturbs molecular adsorption on the SiC nanomesh. When the tip bias was increased to a threshold voltage of +3.3 V, some objects resembling single ClAlPc molecules appear in the initial STM images scanned (not shown). Blurred features dominate such images, indicating a molecule diffusing or hopping heavily. Statistically, an estimated switching probability at the scanning conditions of V_{tip} = 3.3 V, I = 100 pA, and scan speed of 1 s/line is larger than 70%. Upon several (3−5) scans, the images become clear. Figure 4a is a zoomed-out empty states STM image. The area highlighted by a red square was scanned for five times at a positive tip bias of 3.3 V, where individual ClAlPc molecules were observed with an appearance of four lobes enclosing a depression at the center, as shown in the empty states STM image inserted at the top right corner of Figure 4a and in the filled states STM image in Figure 4c. The inset in Figure 4a was taken at the boundary of the red square, highlighting the inconsistent appearance between ClAlPc in- and outside the red square. The ClAlPc molecule in the red square now lies flat on the SiC nanomesh with its Cl atom pointing into the substrate (hereafter, Cl-down configuration). We scanned the same area with a negative tip bias up to −4.0 V and found that the ClAlPc remained in the Cl-down configuration, indicating a weaker tip−molecule interaction in such a configuration. This is indicative of irreversible flipping of ClAlPc induced by the STM tip. Recently, tip-induced single-molecule reversible switching of SnPc on Ag(111) at a temperature lower than 30 K was reported, where the motion of a central Sn ion through the unaffected frame of a phthalocyanine molecule is achieved *via* resonant electron or hole injection into molecular orbitals.[27,28] The same behavior of ClAlPc on graphite was also reported.[29] However, it is not clear here whether the whole ClAlPc molecule

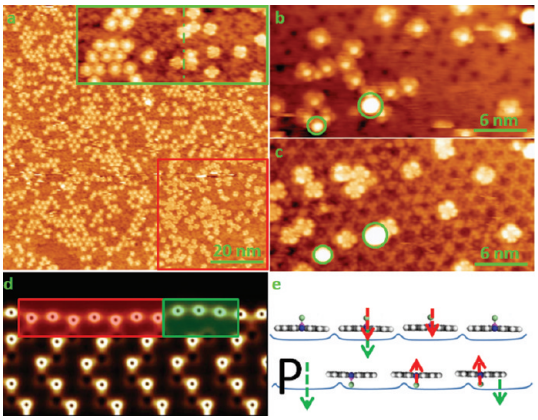

Figure 4. (a) Large scale STM image (V_T = −2.30 V) with ClAlPc molecules in both Cl-up and Cl-down configurations. Area marked by a red square indicates region where scanning at +3.3 V tip bias was carried out for five times, resulting in the molecular configuration inversion from Cl-up to Cl-down. Inset: Zoomed-in STM image (V_T = −2.30 V) over the boundary showing ClAlPc molecules in both Cl-up (left) and Cl-down (right) configurations. STM images from the same area before (b, V_T = −2.60 V) and after (c, V_T = 3.3 V) scanned four times at +3.3 V tip bias for comparison to show that while almost all the Cl-up molecules reside in the holes, the Cl-down molecules reside off the centers of the corresponding host holes and close to the boundary of the nanomesh. (d) Calculated model of SiC nanomesh. (Reprinted with permission from ref 13. Copyright 2008 by American Physical Society). (e) Proposed models and mechanism of ClAlPc in Cl-up and Cl-down configurations on SiC nanomesh. The red arrow indicates the inherent dipole of ClAlPc, the green arrow indicates that of the nanomesh.

flips over or the ClAl-group moves through the frame of a phthalocyanine due to the influence of the positively biased tip. More investigations at lower temperatures are required to elucidate this point.

Figure 4 panels b (V_T = −2.60 V) and c (V_T = 3.30 V) are STM images taken from the same area in higher resolution before and after molecule inversion, where two defects are marked by green circles, respectively, as reference. While all the Cl-up molecules reside at the center of the holes, the Cl-down molecules locate close to the boundaries of the host nanomesh. It can be understood as following. The charge redistribution at a hole of nanomesh (red region in Figure 4d) calculated using density functional theories based on a ($\sqrt{3} \times \sqrt{3}$)R30° unit cell clearly shows electron accumulation (depletion) regions at the carbon layer (SiC substrate). The charge transfer within covalent Si−C bonds is equivalent to nearly one electron per bond (see SI). Since the transferred charge is localized at the carbon layer and located in the nanomesh holes, the out-of-plane components of these induced dipoles point from the carbon layer into SiC, as shown by a green arrow in the proposed model in Figure 4e. The inherent dipole of ClAlPc is indicated by a red arrow. When deposited on SiC nanomesh, ClAlPc in the Cl-up configuration has an inherent downward dipole. This dipole aligns well with that of the nanomesh, which results in an

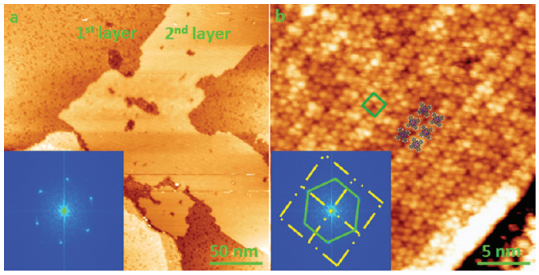

Figure 5. (a) Large scale STM image ($V_T = -3.23$ V) showing the ClAlPc molecules formed a close packed 2nd layer, leaving the molecules in the 1st layer intact. The corresponding FFT pattern shows a hexagonal superstructure and a square superstructure, as highlighted in the inset in panel b. (b) Zoomed-in STM image ($V_T = 2.0$ V) showing the ClAlPc in the 2nd layer arranged in a square arrangement (as marked by a green square) with their Cl atoms pointing toward the substrate. Six ClAlPc molecules were overlaid to guide eyes.

attractive interaction between the ClAlPc and the nanomesh and enhances the stability of the ClAlPc in the center of nanomesh, as shown in the upper panel of Figure 4e. When ClAlPc is inverted to the Cl-down configuration, its inherent dipole is upward and opposite to that of the nanomesh, which results in the off-center adsorption as shown in the lower panel of Figure 4e. Therefore, the downward periodic surface dipole of SiC nanomesh immobilizes molecules with inherent dipoles to form a well-ordered noninteracting single-molecular dipole array.

Upon increasing the coverage of ClAlPc, a closely packed second layer with 4-fold symmetry forms leaving the first layer intact, as shown in Figure 5a. The corresponding FFT pattern inserted at the lower left corner of panel a shows one hexagonal superstructure (from the first layer) and one square superstructure (from the second layer), as highlighted in the same FFT pattern inserted at the lower left corner of panel b. Figure 5b is a close-up image showing the second layer ClAlPc in a square close-packed arrangement with a lattice constant of about 1.50 nm, where ClAlPc appears as four lobes with a center depression (Cl-down configuration). This suggests that the interaction between ClAlPc and nanomesh is strong enough to prevent the insertion of additional ClAlPc molecules into the first layer from forming a close-packed layer. On monolayer EG, ClAlPc molecules in a Cl-up configuration aggregate into a square arrangement with a lattice parameter of ~1.50 nm, suggesting that the effect of SiC nanomesh surface dipoles can be screened by monolayer EG (data not shown).

CONCLUSION

We demonstrate the fabrication of well-ordered ClAlPc molecular dipole arrays on the SiC nanomesh template. The preferential adsorption was steered by the out-of-plane components of the dipole in each nanomesh caused by the unevenly distributed interfacial charge transfer from the SiC to the carbon layer. As revealed by *in situ* LT-STM experiments, ClAlPc molecules adsorb exclusively at the center of the corresponding host SiC nanomesh holes in a Cl-up configuration to form large area well-ordered noninteracting molecular arrays. They can be inverted into a Cl-down configuration under the influence of a positively biased tip with a threshold voltage of 3.3 V, and at the same time, relocate to positions close to the boundary of the host nanomesh. The understanding and fabrication of such large scale well-ordered single-molecule dipole arrays on SiC nanomesh is a first step toward single molecule devices, which could have potential application in the fabrication of other low-dimensional molecular nanostructures with desired functionalities, for example, to anchor other polar functionalized molecules and for use in organic nanodevices. As ClAlPc is switchable between two distinct electric dipole configurations, such dipole arrays hold promise for future ultrahigh density information storage devices and chemical sensors. In addition, it provides a pathway to atomically precise nanopatterning of the ClAlPc and similar dipole molecules on SiC nanomesh.[30]

METHODS

All the experiments were performed in a custom-built multichamber ultrahigh vacuum (UHV) system with base pressure lower than 6.0×10^{-11} mbar, which houses an Omicron LT-STM. The 10 mm × 3 mm SiC sample cut from an as-received n-doped on-axis 4H-SiC(0001) wafer (Cree Inc.) was loaded into the UHV chamber without further treatment and degassed overnight at ~800 °C by resistive heating. After degassing, Si was deposited onto the sample with its temperature kept at ~850 °C to remove the surface oxide. Slowly heating the sample in the absence of a Si flux up to a temperature of 1100 °C or higher resulted in the formation of pure or partially EG covered SiC nanomesh.[11,16] ClAlPc was deposited at ~275 °C from Knudsen cells (MBE Komponenten, Germany) onto SiC nanomesh kept at room temperature in the growth chamber. The deposition rate was calibrated to be ~0.05 ML/min on a pure SiC nanomesh sample. STM imaging was carried out in constant current mode with a chemically etched tungsten (W) tip at 77 K. STM images were analyzed using WSxM.[31]

Conflict of Interest: The authors declare no competing financial interest.

Acknowledgment. We thank Prof. S. Kera at Chiba University (CU) Japan, for kindly providing purified ClAlPc as well as Dr. Y. L. Huang (CU) for fruitful discussion, and acknowledge the support from NRF-CRP Grants R-143-000-360-281: "Graphene and Related Materials and Devices" and R-144-000-295-281: "Novel 2D materials with tailored properties—Beyond graphene", as well as the FRC Grant R-143-000-440-112 and NUS YIA Grant of R143-000-452-101.

Supporting Information Available: Additional figures and information as described in the text. This material is available free of charge *via* the Internet at http://pubs.acs.org.

REFERENCES AND NOTES

1. Aviram, A.; Ranter, M. A. Molecular Rectifiers. *Chem. Phys. Lett.* **1974**, *29*, 277–283.
2. Barth, J. V.; Costantini, G.; Kern, K. Engineering Atomic and Molecular Nanostructures at Surfaces. *Nature* **2005**, *437*, 671–679.
3. Barth, J. V. Molecular Architectonic on Metal Surfaces. *Annu. Rev. Phys. Chem.* **2007**, *58*, 375–407.
4. Zhang, H. L.; Chen, W.; Huang, H.; Chen, L.; Wee, A. T. S. Preferential Trapping of C_{60} in Nanomesh Voids. *J. Am. Chem. Soc.* **2008**, *130*, 2720–2721.
5. Brune, H.; Giovannini, M.; Bromann, K.; Kern, K. Self-Organized Growth of Nanostructure Arrays on Strain-Relief Patterns. *Nature* **1998**, *394*, 451–453.
6. Lin, W. C.; Kuo, C. C.; Luo, M. F.; Song, K. J.; Lin, M. T. Self-Aligned Co Nanoparticle Chains Supported by Single-Crystalline Al_2O_3/NiAl(100) Template. *Appl. Phys. Lett.* **2005**, *86*, 043105−1–043105−3.
7. Hsu, P. J.; Wu, C. B.; Yen, H. Y.; Wong, S. S.; Lin, W. C.; Lin, M. C. Electronically Patterning Through One-Dimensional Nanostripes with High Density of States on Single-Crystalline Al_2O_3 Domain. *Appl. Phys. Lett.* **2008**, *93*, 143104−1–143104−3.
8. Berner, S.; Corso, M.; Widmer, R.; Groening, O.; Laskowski, R.; Blaha, P.; Schwarz, K.; Goriachko, A.; Over, H.; Gsell, S.; *et al.* Boron Nitride Nanomesh: Functionality from a Corrugated Monolayer. *Angew. Chem., Int. Ed.* **2007**, *46*, 5115–5119.
9. Dil, H.; Lobo-Checa, J.; Laskowski, R.; Blaha, P.; Berner, S.; Osterwalder, J.; Greber, T. Surface Trapping of Atoms and Molecules with Dipole Rings. *Science* **2008**, *319*, 1824–1826.
10. Van Bommel, A. J.; Crombeen, J. E.; Van Tooren, A. LEED and Auger Electron Observation of the SiC(0001) Surface. *Surf. Sci.* **1975**, *48*, 463–472.
11. Chen, W.; Xu, H.; Liu, L.; Gao, X. Y.; Qi, D. C.; Peng, G. W.; Tan, S. C.; Feng, Y. P.; Loh, K. P.; Wee, A. T. S. Atomic Structure of the 6H-SiC(0001) Nanomesh. *Surf. Sci.* **2005**, *596*, 176–186.
12. Martensson, P.; Owman, F.; Johansson, L. I. Morphology, Atomic and Electronic Structure of 6H-SiC(0001) Surfaces. *Phys. Stat. sol. (b)* **1997**, *202*, 501–528.
13. Varchon, F.; Mallet, P.; Veuillen, J. Y.; Magaud, L. Ripples in Epitaxial Graphene on the Si-terminated SiC(0001) Surface. *Phys. Rev. B* **2008**, *77*, 235412-1–235412-8.
14. Kim, S.; Ihm, J.; Choi, H. J.; Son, Y. W. Origin of Anomalous Electronic Structures of Epitaxial Graphene on Silicon Carbide. *Phys. Rev. Lett.* **2008**, *100*, 176802−1–176802−4.
15. Emtsev, K. V.; Speck, F.; Seyller, Th.; Ley, L.; Riley, J. D. Interaction, growth, and ordering of epitaxial graphene on SiC(0001) surfaces: A comparative photoelectron spectroscopy study. *Phys. Rev. B.* **2008**, *77*, 155303−1–155303−10.
16. Huang, H.; Chen, W.; Chen, S.; Wee, A. T. S. Bottom-up Growth of Epitaxial Graphene on 6H-SiC(0001). *ACS Nano* **2008**, *2*, 2513–2518.
17. Kubler, L.; Ait-Mansour, K.; Diani, M.; Dentel, D.; Bischoff, J. L.; Derivaz, M. Bidimensional Intercalation of Ge between SiC(0001) and a Heteroepitaxial Graphite Top Layer. *Phys. Rev. B* **2005**, *72*, 115319−1–115319−10.
18. Riedl, C.; Coletti, C.; Iwasali, T.; Zakharov, A. A.; Starke, U. Quasi-Free-Standing Epitaxial Graphene on SiC Obtained by Hydrogen Intercalation. *Phys. Rev. Lett.* **2009**, *103*, 246804−1–246804−4.
19. Gierz, I.; Suzuki, T.; Lee, D. S.; Krauss, B.; Riedl, C.; Starke, U.; Hochst, H.; Smet, J. H.; Ast, C. R.; Kern., K. Electronic Decoupling of an Epitaxial Graphene Monolayer by Gold Intercalation. *Phys. Rev. B* **2010**, *81*, 235408−1–235408−6.
20. Oida, S.; McFeely, F. R.; Hannon, J. B.; Tromp, R. M.; Copel, M.; Chen, Z.; Sun, Y.; Farmer, D. B.; Yurkas, J. Decoupling Graphene from SiC(0001) *via* Oxidation. *Phys. Rev. B* **2010**, *82*, 041411−1–041411−4.
21. Virojanadara, C.; Watcharinyanon, S.; Zakharov, A. A.; Johansson, L. I. Epitaxial Graphene on 6H-SiC and Li Intercalation. *Phys. Rev. B* **2010**, *82*, 205402−1–205402−6.
22. Wong, S. L.; Huang, H.; Wang, Y.; Cao, L.; Qi, D.; Santoso, I.; Chen, W.; Wee, A. T. S. Quasi-Free-Standing Epitaxial Graphene on SiC (0001) by Fluorine Intercalation from a Molecular Source. *ACS Nano* **2011**, *5*, 7662–7668.
23. Chen, S.; Chen, W.; Huang, H.; Gao, X. Y.; Qi, D. C.; Wang, Y. Z.; Wee, A. T. S. Template-Directed Molecular Assembly on Silicon Carbide Nanomesh: Comparison Between CuPc and Pentacene. *ACS Nano* **2010**, *4*, 849–854.
24. Kera, S.; Yamane, H.; Honda, H.; Fukagawa, H.; Okudaira, K. K.; Ueno, N. Photoelectron Fine Structures of Uppermost Valence Band for Well-Characterized ClAl-Phthalocyanine Ultrathin Film: UPS and MAES Study. *Surf. Sci.* **2004**, *566*, 571–578.
25. Owman, F.; Martensson, P. The SiC(0001) $6\sqrt{3} \times 6\sqrt{3}$ Reconstruction Studied with STM and LEED. *Surf. Sci.* **1996**, *369*, 126–136.
26. Huang, Y. L.; Wang, R.; Niu, T. C.; Kera, S.; Ueno, N.; Pflaum, J.; Wee, A. T. S.; Chen, W. One Dimensional Molecular Dipole Chain Arrays on Graphite *via* Nanoscale Phase Separation. *Chem. Commun.* **2010**, *46*, 9040–9042.
27. Wang, Y. F.; Kroger, J.; Berndt, R.; Hofer, W. A. Pushing and Pulling a Sn Ion through an Adsorbed Phthalocyanine Molecule. *J. Am. Chem. Soc.* **2009**, *131*, 3639–3643.
28. Toader, M.; Hietschold, M. Tuning the Energy Level Alignment at the SnPc/Ag(111) Interface Using an STM Tip. *J. Phys. Chem. C* **2011**, *115*, 3099–3105.
29. Huang, Y. L.; Lu, Y. H.; Niu, T. C.; Huang, H.; Kera, S.; Ueno, N.; Wee, A. T. S.; Chen, W. Reversible Single-Molecule Switching in an Ordered Molecular Dipole Array. *Small* **2012**, 10.1002/smll.201101967.
30. Wang, Q. H.; Hersam, M. C. Nanofabrication of Heteromolecular Organic Nanostructures on Epitaxial Graphene *via* Room Temperature Feedback-controlled Lithography. *Nano Lett.* **2011**, *11*, 589–593.
31. Horcas, I.; Fernandez, R.; Gomez-Rodriguez, J. M.; Colchero, J. WSXM: A Software for Scanning Probe Microscopy and a Tool for Nanotechnology. *Rev. Sci. Instrum.* **2007**, *78*, 013705−1–013705−8.